Sensory innervation of masseter, temporal and lateral pterygoid muscles in common marmosets

Anahit H. Hovhannisyan[1], Karen A. Lindquist[5], Sergei Belugin[1], Jennifer Mecklenburg[1], Jaclyn Merlo[1], Meilinn Tram[1,5], Tatiana M. Corey[4], Adam B. Salmon[3,6,7], Daniel Perez[8], Shivani Ruparel[1,2,5] and Armen N. Akopian[1,2,5 *]

Departments of [1]Endodontics, [2]Pharmacology, [3]Molecular Medicine, [4]Laboratory Animal Resources and [8]Oral and Maxillofacial Surgery, University of Texas Health Science Center at San Antonio, San Antonio, Texas 78229

[5]Integrated Biomedical Sciences (IBMS) Program, University of Texas Health Science Center at San Antonio, San Antonio, Texas 78229

[6]Sam and Ann Barshop Institute for Longevity and Aging Studies, The University of Texas Health Science Center at San Antonio, San Antonio, Texas, USA 78229

[7]South Texas Veterans Health Care System, Geriatric Research Education and Clinical Center San Antonio, TX, USA 78229

***Corresponding authors:**

Armen N. Akopian

The School of Dentistry, University of Texas Health Science Center @ San Antonio

7703 Floyd Curl Drive, San Antonio, TX 78229-3900

Office: (210) 567-3193 Fax: (210) 567-3389 Email: Akopian@UTHSCSA.edu

Abstract

Myogenous temporomandibular disorders (TMD-M) are the most prevalent group of painful orofacial conditions, and the second most frequent among musculoskeletal pain conditions. TMD-M is associated with an increased responsiveness of nerves innervating the masseter (MM), temporal (TM), medial pterygoid closing (MPM) and lateral pterygoid gliding muscles (LPM). Treatment of this disorder remains difficult and is further complicated by each muscle having diverse and functionally distinct nerve innervation. This study examined expression of sensory markers in MM, TM and LPM of adult male common marmosets, a type of non-human primate. Using immunohistochemistry, we found that masticatory muscles were predominantly innervated with A-fibers (NFH^+). All C-fibers ($pgp9.5^+/NFH^-$) observed in masticatory muscles were peptidergic ($CGRP^+$) and lacked antibody labeling for mrgprD, trpV1 and the silent nociceptive marker – CHRNA3. The proportion of C- to A-fibers was highest in LPM, while MM had a minimal percentage (6-8%) of C-fibers. Interestingly, C-fibers in masticatory muscle may have myelin sheath, since many NFH^- nerves were labeled with $GFAP^+$. A-fiber types were also dissimilar among these muscles. Thus, there are substantially more peptidergic A-fibers ($CGRP^+/NFH^+$) in TM and LPM compared to MM. Almost all A-fibers in MM expressed trkC, with some of them having trkB and parvalbumin (PV). In contrast, a lesser number of TM and LPM nerves expressed trkC, lacked trkB and had fewer PV^+ fibers in LPM. Along with sensory fibers, the masticatory muscles contain sympathetic fibers (tyrosine hydroxylase; TH^+), which are located around blood vessels. This TH expression was absent in trigeminal neurons. Overall, the masticatory muscles of male marmosets have distinct expression patterns when compared to each muscle of the jaw and cutaneous fibers innervated by DRG neurons.

Keywords

Myogenous temporomandibular disorders (TMD-M), trigeminal nerves, masseter muscle, temporal muscle, lateral pterygoid muscle, nonhuman primate, common marmoset

Abbreviations

TG – trigeminal ganglia

TMD-M - myogenous temporomandibular disorder

TMJ - temporomandibular joint

V1 – ophthalmic nerve of trigeminal ganglia

V2 – maxillary nerve of trigeminal ganglia

V3 – mandibular nerve of trigeminal ganglia

MN – masseteric nerve

ATN - auriculotemporal nerve

TN – posterior deep temporal nerve

TJM nerve – TJM branch of mandibular nerve

LPM - lateral pterygoid muscle

MPM - medial pterygoid muscles

MM – masseter muscle

TM – temporal muscle

Introduction

Myogenous temporomandibular disorders (TMD-M) are the most prevalent group of painful orofacial conditions (Dworkin and Massoth, 1994; Manfredini et al., 2011; Treede et al., 2015). Among musculoskeletal chronic pain conditions, TMD-M is the second most widespread after chronic low back pain (Meloto et al., 2019). Unlike well-localized cutaneous pain, TMD-M is often manifested as referred pain to other deep tissues (i.e. toothache, headache) (Mense, 2003). Current knowledge on TMD-M related pain mechanisms is limited and further understanding is confounded by conflicting evidence concerning changes in superficial sensitivity seen in patients with craniofacial myalgia (Svensson and Graven-Nielsen, 2001). Thus, TMD-M is rarely accompanied by clinical signs and histopathologic evidence of injury or inflammation (Ettlin et al., 2021). Therefore, some studies (Kosek et al., 2016) have classified TMD-M as nociplastic pain (Cayrol et al., 2022). Despite these debatable points, there is an agreement that TMD-M leads to sensitization of nociceptive and non-nociceptive trigeminal ganglia (TG) sensory neurons innervating the masticatory muscles, leading to increase signal input into the central nervous system (Fitzcharles et al., 2021).

Increased responsiveness of sensory neurons during TMD-M could occur in any muscle controlling temporomandibular joint (TMJ) articulation, including superficial and in the deep heads of masseter muscle (MM), temporal muscle (TM), medial pterygoid closing muscles (MPM) as well as gliding superior and inferior heads of the lateral pterygoid muscles (LPM) (Kucukguven et al., 2022; Nickel et al., 2022) (*Fig 1*). Muscle tissues of the TMJ structure are innervated by the masseteric nerve (MN) for MM, the auriculotemporal nerve (ATN) for LPM, and temporal nerve (TN) for TM (*Fig 1*). In the pathophysiology of TMD-M pain and mastication muscle innervation, past studies have focused on the ATN (Johansson et al., 1990). However, some studies have indicated that the MN and posterior deep TN can also undergo sensitization during TMD-M (Davidson et al., 2003) (*Fig 1*).

Unlike the inferior alveolar nerve (Tsuboi et al., 2015; Tsuboi et al., 2004), ATN, MN, TN and TMJ nerves are almost uncharacterized and there is only scant information on the types of afferent fibers and their function and plasticity within these branches of the mandibular (V3) nerve. The existing data was generated via extracellular recordings from the submandibular and buccal regions, which are innervated by the ATN. Recordings indicate that ATN may contain C-fibers and slow adapting A-fibers (Furusawa et al., 1993; Nonaka et al., 2001; Oka et al., 2001). Electrophysiological characterization and immunohistochemistry with sensory nerve fiber markers showed that mouse MM is almost exclusively innervated by myelinated fibers (Lindquist et al., 2021). To properly understand and treat TMD-M pain further knowledge of the type of peripheral sensory innervation in the masticatory muscles is crucial.

We and others have demonstrated that expression patterns and characteristics of dorsal root (DRG) and TG sensory neurons depends on innervation targets (Hockley et al., 2019; Lindquist et al., 2021; Wu et al., 2018). Moreover, there is significant differences in transcriptomic profiles of sensory neurons between rodents and humans (Nguyen et al., 2021; Tavares-Ferreira et al., 2022; Yang et al., 2022). These critical differences could explain to some extent why translation of findings in rodents to clinical settings has been challenging, and stresses the need to further investigate sensory systems in other species that might better model the human anatomy and function. In this respect, nonhuman primate (NHP) models are of particular interest for additional pre-clinical testing towards translation. In this study, we used common marmosets (Callithrix jacchus), a well-characterized new world monkey used commonly for research across multiple fields including toxicology, neurological diseases, reproductive biology and aging. We report on immunohistochemistry (IHC) and known molecular markers of sensory nerve types used to characterize and identify the neuroanatomical distributions of these fibers in MM, TM and LPM of naïve adult male common marmosets.

Material and methods

Animals and ethical approval

For our studies, we collected tissue from 4-11 adult male marmosets for all experiments. Animals were housed at the University of Texas Health Science Center at San Antonio (UTHSCSA) or Texas Biomedical Research Institute (TBRI, San Antonio, TX). All animal experiments conformed to IASP and APS's Guiding Principles in the Care and Use of Vertebrate Animals in Research and Training. We also followed guidelines issued by the National Institutes of Health (NIH) and the Society for Neuroscience (SfN) to minimize the number of animals used and their suffering. All animals were maintained on approved protocols by the respective Institutional Animal Care and Use Committees (IACUC). Samples for this study were collected opportunistically from animals that were euthanized at IACUC approved endpoints on their respective studies.

Tissue collection and Processing

Animals were euthanized by the veterinarians in UTHSCSA and TBRI at defined end points that were determined for each animal. At the point of determined death, superficial and deep heads of MM, TM, superior and inferior heads of LPM with attached TMJ ligament, trigeminal ganglia (TG), hindpaw skin and tongue were dissected and placed in 4% paraformaldehyde (PFA). Tissues were fixed in 4% PFA for 3-4 hours, washed in 3 × 15 min in 0.1M Phosphate Buffer (PB), equilibrated in 10% sucrose in PB at 4°C overnight and cryo-protected and stored in 30% sucrose in PB at −20°C. Tissues were embedded in Neg 50 (Richard Allan Scientific, Kalamazoo, MI); and were cryo-sectioned with the following thickness: TG 20 μm and MM, TM and LPM 30 μm.

Immunohistochemistry (IHC)

Immunostaining was performed as described previously (Belugin et al., 2013; Patil et al., 2019). Briefly, sections were blocked in 4% normal donkey serum (Sigma, St. Louis, MO), 2%

bovine gamma-globulin (Sigma-Aldrich, St. Louis, MO) and 0.3% Triton X-100 (Fisher Scientific) in 0.1M PBS for 90 min at RT. Next, tissue sections were incubated for 24-36 hours at RT with primary antibodies. Sections were washed with PBS from unbound primary antibodies, blocked, and incubated for 90 min at RT with appropriate fluorophore conjugated secondary antibodies (Jackson Immuno-Research, West Grove, PA, USA). Finally, tissue sections were washed for 3 x 5 minutes with 0.1M PBS and 2 x 5 minutes in diH_2O, air-dried, and covered with Vectashield Antifade Mounting Medium (Vectorlabs, Burlingame, CA, USA). In this study, the following previously characterized primary antibodies were used: anti-PGP9.5 rabbit polyclonal (Millipore-Sigma; Burlington, NJ, catalog AB1761-I; 1:300) (Boyd et al., 2021); anti-Neurofilament H (NF-H) chicken polyclonal (BioLegend; San Diego, CA; catalog 822601; 1:1000) (Avona et al., 2021); anti-CGRP guinea pig polyclonal (Synaptic Systems; Goettingen, Germany; catalog 414 004; 1:200) (Samms et al., 2022); anti-TRPV1 rabbit polyclonal (Novus Biologicals; Centennial, CO; catalog NBP1-71774SS; 1:200) (Moutafidi et al., 2021); anti-mrgprD rabbit polyclonal (Alamone Lab; catalog ASR-031; 1:200) (de Carvalho Santuchi et al., 2019; Lindquist et al., 2021); anti-CHRNA3 rabbit polyclonal (Bioss; catalog BS-6455R; 1:200) (He et al., 2014); anti-tyrosine hydroxylase (TH) chicken polyclonal (Neuromics; Bloomington, MN; catalog CH23006; 1:300) (Ferreira-Pinto et al., 2021); anti-smooth muscle actin (α-SMA) Cy3-conjugated rabbit polyclonal antibody (Millipore-Sigma; catalog C6198; 1:500); anti-trkC rabbit polyclonal (Aviva Systems Biology, San Diego, CA; catalog ARP51318_P050; 1:200); anti-trkB goat polyclonal (R&D systems; AF1494; 1:200) (Arcourt et al., 2017); anti-parvalbumin rabbit polyclonal (Novus Biologicals; catalogue NB120-11427SS; 1:200) (Lewis et al., 2021); anti-calbindin D28k rabbit polyclonal (Synaptic Systems; catalogue 214 011; 1:200) (Navarro-Gonzalez et al., 2021).

Counting of Fibers and Neurons:

Images were acquired using a Keyence BZ-X810 all-in-one microscope (Itasca, IL, USA) in the “sectioning” mode. Images were acquired with a 10× or 20× objective. Settings were

determined in such way that no-primary control did not show any positive signal. Then, images were taken using these fixed acquisition parameters across all groups. Control IHC was performed on tissue sections processed as described but either lacking primary antibodies or lacking primary and secondary antibodies. Z-stack IHC images were obtained from 3-5 independent tissue sections from 2-3 isolations. Mean values from these 3-5 sections generated from an isolation represented data for a biological replicate. Thus, these 2-3 isolations represent the biological replicates *(*i.e. *n*). Neuronal fibers were counted manually using Image J software to obtain approximate estimation of the density of peripheral innervation of muscle tissues with the nerve fibers expressing specific markers. Bundles of fibers grouped together that couldn't be visually separated were also counted as 1.

Statistical Analyses

GraphPad Prism 8.0 (GraphPad, La Jolla, CA) was used for statistical analysis. Data are presented as mean ± standard error of mean (SEM). Differences between groups were assessed by chi-square analysis with Fisher's exact test, unpaired t-test, or 1-way ANOVA with Bonferroni's post-hoc test. A difference is accepted as statistically significant when $p<0.05$. Interaction F ratios, and the associated p values are reported.

Results

Expression of C- and A-fibers in the masticatory muscles.

To examine the proportion of C-fibers compared to A-fibers in male marmoset masticatory muscles, we labeled A-fibers with NFH (Henry et al., 2012; Lawson and Waddell, 1991) and all sensory fibers with pgp9.5 (Day and Thompson, 2010; Henry et al., 2012). Pgp9.5^{+} and NFH^{+} fibers were detected throughout MM, but the junction of superficial and deep heads of MM was more densely labeled. Similar innervation pattern was observed in mouse MM (Lindquist et al., 2021). In

contrast, both Pgp9.5$^+$ and NFH$^+$ fibers were evenly distributed throughout TM and LPM. Superior and inferior LPM were also contained approximately equal numbers of Pgp9.5$^+$ and NFH$^+$ fibers.

NFH and pgp9.5 labeling overlapped in a majority of sensory nerves in MM (*Fig 2*). TM and LPM had substantially more proportion of C-fibers (pgp9.5$^+$/NFH$^-$) compared to MM (*Figs 2, 3A*; 1-way ANOVA; F (2, 4) = 44.48; P=0.002; n=2-3). Thus, we calculate that MM had ≈8% C-fibers and 92% A-fibers, while TM and LPM had ≈30-35% C-fibers and 65-70% A-fibers (*Fig 3A*). Overall, mastication muscles were found to be predominantly innervated by A-fibers. MM contained the highest proportion of A-fibers, whereas LPM had lowest.

A-fibers are considered myelinated, while C-fibers are unmyelinated (Henry et al., 2012). To examine whether this is the case for sensory nerves in masticatory muscles of adult marmosets, we labeled myelinated fibers with GFAP antibodies, which were validated in marmosets trigeminal ganglia (TG) (*Suppl Fig 1*) (Marinkovic et al., 2009). All NFH$^+$ nerves in MM were labeled with GFAP, but about 4% nerves were GFAP$^+$/NFH$^-$ (*Figs 3B, 4*). NFH$^+$ nerves in TM and LPM were also co-labeled with GFAP (*Fig 4*). Proportions of GFAP$^+$/NFH$^-$ fibers in TM and, especially LPM were significantly higher compared to MM (*Figs 3B, 4*; 1-way ANOVA; F (2, 4) = 20.03; P=0.008; n=2-3). We found that TM and LPM contained ≈28% and ≈43% GFAP$^+$/NFH$^-$ fibers, respectively (*Fig 3B*). Altogether, the masticatory muscles contain a subset (lowest percentage in MM and highest in LPM) of myelinated C-fibers. These myelinated C-fibers could represent bundles of nerves wrapped with myelin sheathes, which were observed in dura mater (Andres et al., 1987).

Expression of CGRP$^+$ peptidergic nerves in the masticatory muscles.

A standard marker for peptidergic nerves and neurons is CGRP (Patil et al., 2018; Usoskin et al., 2015). We used validated anti-CGRP antibodies, which exhibited strong labeling in a subset of TG neurons in adult male marmosets (*Suppl Fig 1*). Compared to CGRP$^+$ signal strength in marmosets TG, CGRP$^+$ labeling in masticatory muscle was significantly dimmer (*Fig 5 and Suppl Fig 1*). MM had about 23% of CGRP$^+$ nerves, and among them, only ≈3% were CGRP$^+$/NFH$^-$ (*Figs*

3A, 5). The proportion of CGRP$^+$ fibers were higher in TM and particularly in LPM compared to MM (*Figs 3A, 5*; 1-way ANOVA; F (2, 4) = 24.30; P=0.006; n=2-3). Nevertheless, less than half of CGRP$^+$ positive fibers were GFAP$^+$/NFH$^-$ in TM and LPM (*Fig 3A*). These data indicate that peptidergic nerves in the masticatory muscles, especially MM, are predominantly composed of A-fibers.

Expression of C-fiber markers in the masticatory muscles.

Data from *Figures 1-5* imply that masticatory muscles have relatively smaller subset of C-fibers compared to skin and dura mater and are predominantly innervated by A-fibers (Andres et al., 1987; Melo-Carrillo et al., 2017; Welk et al., 1990). Here, we have evaluated expression of several markers of C-fibers in the masticatory muscles. Antibodies for trpV1 did not detect positive fibers in MM and TM (*Figs 3A, 6, 7*). However, about 10-12% of nerves in LPM showed trpV1 labeling (*Figs 3A, 7*). Interestingly, all trpV1$^+$ nerves were bundled and co-labeled with NFH. A similar pattern was observed for mrgprD, a marker for non-peptidergic nerves (Patil et al., 2018; Usoskin et al., 2015), with about 10-12% of nerves in LPM being MrgrprD$^+$ fibers, which were bundled and co-labeled with NFH (*Fig 3A, 7*). Overall, we found that MM and TM did not show immunoreactivity for trpV1$^+$ or non-peptidergic sensory fibers, whereas LPM contained both trpV1$^+$ and MrgrprD$^+$ fibers, which were bundled and co-labeled with NFH. This unusual expression pattern could imply that LPM is not innervated by trpV1$^+$ and MrgrprD$^+$ fibers. Whereas bundled trpV1, MrgrprD and NFH nerves may belong to a branch of the ATN nerve trunk, which passes through LPM towards the TMJ ligament.

Nociceptors responsive to very high-threshold *in vitro* or *in vivo* mechanical stimuli or insensitive to piezo device stimulation have been termed “silent” nociceptors. These nociceptors are a subset of C-fibers in DRG and identified by the nicotinic acetylcholine receptor subunit alpha-3 (CHRNA3) (Prato et al., 2017). We used validated anti-CHRNA3 antibodies, which show labeling of fibers in the togue of common marmosets (*Suppl Fig 1*), to identify CHRNA3$^+$ fibers in mastication

muscles. Unlike NPH tongue, MM, TM and LPM did not express CHRNA3 nerves at a detectable level (*Figs 6, 7*).

Expression of A-fiber markers in the masticatory muscles.

Single-cell RNA sequencing data and electrophysiology studies on reporter mice indicate that tyrosine hydroxylase (TH), trkB, trkC, parvalbumin (PV) and calbindin-28d (Calb) are markers for DRG low-threshold mechanoreceptor (LTMR) sensory neurons and cutaneous A-fibers (Bai et al., 2015; Li et al., 2011; Patil et al., 2018; Usoskin et al., 2015). Validated antibodies for trkB, trkC, PV and Calb labeled a subset of TG neurons in marmosets (*Suppl Fig 2*), whereas we observed no TH labeling of neurons or non-neuronal cells in marmosets TG (*Suppl Fig 1*). TrkB as a marker for Aδ-LTMR in skin labeled about 22% of NFH^+ fibers in MM (*Figs 3A, 8*) (Rutlin et al., 2014). In contrast, TM and LPM did not have detectable trkB labeling (*Figs 3A, 9*; 1-way ANOVA; F (2, 4) = 105.0; P=0.0003; n=2-3). A marker for Aβ-LTMR, trkC, was present on a majority of NFH^+ fibers in MM (*Figs 3A, 8*) (Li et al., 2011; Usoskin et al., 2015). However, trkC was identified only in a subset of A-fibers in TM and LPM (*Fig 9* and *Suppl Fig 3*). The percentages of $trkC^+$ A-fibers in TM and LPM were significantly less than those found in the MM (*Figs 3A, 8, 9*; 1-way ANOVA; F (2, 4) = 54.95; P=0.0012; n=2-3). Certain $trkC^-/NFH^+$ and $trkC^+/NFH^+$ fibers were located at the junction of muscle and tendon in TM (*Suppl Fig 3*). PV is another traditional marker for certain Aβ-LTMR and proprioceptors in DRG (Li et al., 2011; Usoskin et al., 2015). PV^+ fibers were present among NFH^+ nerves in MM and TM, and to a lesser extent in LPM (*Figs 3A, 8, 9*; 1-way ANOVA; F (2, 4) = 24.02; P=0.006; n=2-3). Calb expression was detected in the Aβ-field (aka NF2) sensory neuron type (Kupari et al., 2021; Sharma et al., 2020; Usoskin et al., 2015). $Calb^+$ nerves were not found in MM, TM or LPM (*Figs 3A, 8, 9*). Overall, MM, TM and LPM have unique subsets of A-fibers, which are defined by expression patterns of trkB, trkC, Calb and PV.

TH is a marker for cutaneous C-LTMR (Li et al., 2011; Seal et al., 2009). We could not identify TH^+ sensory neurons in marmosets TG (*Suppl Fig 1*). However, widespread TH^+ innervation was revealed in the masticatory muscles (*Figs 3B, 10*). The number of TH^+ fibers were slightly more compared to NFH^+ ones in all studied masticatory muscles (*Figs 3A, 10*; 1-way ANOVA; $F(2, 4) = 0.95$; $P=0.46$; n=2-3). A majority of TH^+ fibers were not co-localized with NFH, but positioned around alpha-smooth muscle actin (α-SMA^+) blood vessels in MM, TM and LPM (*Figs 3A, 10*; 1-way ANOVA; $F(2, 4) = 0.45$; $P=0.67$). Overall, our data suggest that the masticatory muscles are innervated by A-LTMR. Types of A-LTMR are unique for each of these muscles and MM had the highest proportion of A-LTMR among NFH^+ nerves. TH^+ C-LTMR nerves were absent in the masticatory muscles, and no TH^+ neurons have been identified in TG. This indicates that TH^+ nerves around blood vessels in MM, TM and LPM probably represent sympathetic fibers.

Discussion

The etiology and pathogenesis of myogenous TMD (TMD-M) and its prevalence in women is poorly understood (Chisnoiu et al., 2015; Kristensen et al., 2016; Svensson and Graven-Nielsen, 2001). However, there is an agreement that TMD-M leads to sensitization of nociceptive and non-nociceptive TG sensory neurons innervating the masticatory muscles, and thereby enhancing signal input into the central nervous system and inducing pain (Fitzcharles et al., 2021). Thus, in order to improve our knowledge about chronic TMD-M and possible therapeutic targets, it is essential to characterize sensory nerves in the masticatory muscles. Such information will have higher translatability to clinical application when it is obtained from either humans or animal models that have similar neuroanatomy to humans. Accordingly, the main aim of this study was to use sensory neuronal markers for identifying sensory nerve fibers innervating the masticatory muscles of common marmosets, a nonhuman primate species that more closely represents human physiology, genetics, and anatomy than do rodent models.

Current single-cell RNA sequencing data imply that DRG and TG sensory neurons have similar neuronal clusters (Nguyen et al., 2017; Sharma et al., 2020; Yang et al., 2022). However, it was demonstrated for several tissues that expression patterns for a variety of genes and electrical activity of DRG and TG sensory neurons depends on innervation targets (Hockley et al., 2019; Lindquist et al., 2021; Wu et al., 2018). Hence, we have selected key masticatory muscles, MM, TM and LPM, for this study. These muscles, especially MM, contained a substantially higher proportion of A relatively to C-fibers (*Fig 11*). This innervation pattern is similar to those observed in mouse MM, which is almost exclusively innervated by A-fibers (Lindquist et al., 2021). C-fibers in the masticatory muscles of adult male marmosets are peptidergic, lack non-peptidergic neuronal marker mrgprD and not labeled with trpV1 antibodies. Masticatory muscles also lack the marker for the "silent" nociceptor, CHRNA3 (Prato et al., 2017). Absence of mrgprD+ and trpV1^{+} immunoreactivities and lack of trpV1-GFP^{+} and mrgprD-TdTom^{+} nerves were also reported in mouse MM (Lindquist et al., 2021). Nonetheless, we observed mrgprD^{+} and trpV1^{+} fibers together with NFH^{+} ones in LPM, while mrgprD^{+}/NFH^{-} and trpV1^{+}/NFH^{-} nerves were absent in LPM. This phenomenon could be explained by the fact that LPM is innervated by a mandibular nerve branch - ATN, which travels through LPM on the way to innervating TMJ ligaments (Kucukguven et al., 2022). Therefore trpV1, mrgprD and NFH could belong to such a nerve trunk targeting TMJ. It could be noted that behavioral experiments on rodents and clinical data demonstrated that intramuscular capsaicin (>10μg) elicits nociception in rodents and pain and crump-like sensation for humans (Joseph et al., 2019; Lee et al., 2009; Melo-Carrillo et al., 2017; Ro and Capra, 2006; Srbely et al., 2010). One of possible explanations for this difference is that low levels of trpV1 on nerves is sufficient for responses to capsaicin stimulation, while substantially higher expression of trpV1 on fibers is required to reveal immunoreactivity. Another possibility is that trpV1 is expressed on non-neuronal cells surrounding sensory fibers.

Data from single-cell RNA sequencing from primate DRG neurons imply that masticatory muscle C-fibers are not similar to PEP1 group containing trpV1. PEP2 and PEP3 sensory neuronal

groups are peptidergic with no trpV1 expression (Kupari et al., 2021). However, PEP2 and PEP3 represent A-fibers and are similar to mouse CGRP-eta (Kupari et al., 2021; Sharma et al., 2020). Considering that primate masticatory muscles have NFH^+ peptidergic fibers, which probably belong to the A-HTMR group (Patil et al., 2018; Sharma et al., 2020) (*Fig 11*), identity of C-fibers in these muscles are not clear.

. The remaining A-fibers could be classified as A-LTMR (Li et al., 2011) (*Fig 11*). MM, TM and LPM have no expression of Calbindin, which is a marker for NF2 cluster in DRG sensory neurons (Usoskin et al., 2015). The cutaneous Aδ-LTMR marker, TrkB, was found only expressed in MM at low levels (*Fig 11*), and most likely has a distinct function when compared to Aδ-LTMR fibers innervating hair (Bai et al., 2015; Rutlin et al., 2014). Parvalbumin is a marker for Aβ-LTMR and was present in few nerves of masticatory muscles. Dominant marker for A-LTMR in MM, TM and LPM was shown to be trkC (*Fig 11*). Altogether, innervation of the masticatory muscles in marmosets is clearly distinct from cutaneous fibers and primate DRG neurons. Thus, it is not clear whether A-LTMR in masticatory muscles terminate in specialized cell structures, such as Merkel cells, Messner or Pacinian corpuscles as they do in skin. However, there is a similarity between MM innervation in primates versus mice (Lindquist et al., 2021). Nevertheless, we also noted substantial differences in nerve types between MM, TM and LPM. These differences can be precisely identified only by detailed single-cell RNA sequencing.

C-fibers are traditionally considered un-myelinated fibers. However, it was noted that several C-fibers could compose a nerve trunk, which is wrapped in a myelin sheath (Andres et al., 1987). Our data imply that C-fibers in the masticatory muscles are also wrapped in myelin sheath, which can be detected by labelling with GFAP. Precise organization of C-fibers in these muscles will need to be uncovered using electron microscopy. C-fibers could lose $GFAP^+$ sheath during last 30-100μm stretch before innervating targets as they do in dura mater (Andres et al., 1987). Primate TG neurons also lack TH labeling in TG. It may indicate that the masticatory muscles do not have C-

LTMR. On other hand, extensive network of TH^+ fibers, which do not co-localize with NFH fibers was detected around blood vessels in MM, TM and LPM. One possible identities for such TH+ fibers are sympathetic nerves.

Conclusions

The main conclusions of this study are that (1) the nerves innervating marmoset masticatory muscle are unique compared to cutaneous nerves; (2) innervation nerve subgrouping depend on masticatory muscle types; (3) distinct masticatory nerves (MN, TM, ATN and TMJ-nerve) may have differing electrical properties at normal and pathological conditions such as many sub-types of TMD; (4) information available thus far suggests that NHP primate and mouse nerves innervating MM could be quite similar; and (5) highest genetic association of PEP1 and NP2 to human pain states may not apply for TMD-M (Kupari et al., 2021).

Declaration of Competing Interest

The authors declare that they have no known competing financial interests or personal relationships that could influence the work reported in this paper.

Acknowledgements

We would like to thank Dr. Christopher Chen (Texas Biomedical Research Institute, San Antonio, TX) for his advice in working with primate tissues, Dr. Corina Ross in helping obtain primate tissues via the tissue share program at Southwest National Primate Research Center (SNPRC), San Antonio, TX, the veterinarians of SNPRC with help in dissection of tissues, and Mrs. Qun Li and Mrs. Fang-Mei Chang for validation of trpV1 and CGRP antibodies for human/primate tissues.

Funding

This work was supported by National Institutes of Health (NIH)/NIDCR The Helping to End Addiction Long-term (HEAL) Initiative (grants DE029187 to A.N.A. and S.R. and DE029187-01S1 to A.N.A. and S.R.); and NIH/NIAMS HEAL Initiative, The Restoring Joint Health and Function to Reduce Pain (RE-JOIN) Consortium (grants AR082195 to A.N.A.).

Author contribution:

A.H.H and K.A.L. conducted a majority of experiments and analysis; S.B., J.M., J.M. and M.T. performed certain experiments and analysis; S.B., J.M., M.T. contributed to tissues preparation; T.M.C., A.B.S. and D.P. performed tissue isolation; D.P., S.R. and A.N.A. analyzed data, edited draft and the final version of the manuscript; A.N.A. designed and directed the project, wrote the first draft of the manuscript; and prepared the final version of the manuscript.

Reference:

Andres, K.H., von During, M., Muszynski, K., and Schmidt, R.F. (1987). Nerve fibres and their terminals of the dura mater encephali of the rat. Anat Embryol (Berl) *175*, 289-301.

Arcourt, A., Gorham, L., Dhandapani, R., Prato, V., Taberner, F.J., Wende, H., Gangadharan, V., Birchmeier, C., Heppenstall, P.A., and Lechner, S.G. (2017). Touch Receptor-Derived Sensory Information Alleviates Acute Pain Signaling and Fine-Tunes Nociceptive Reflex Coordination. Neuron *93*, 179-193.

Avona, A., Mason, B.N., Burgos-Vega, C., Hovhannisyan, A.H., Belugin, S.N., Mecklenburg, J., Goffin, V., Wajahat, N., Price, T.J., Akopian, A.N.*, et al.* (2021). Meningeal CGRP-Prolactin Interaction Evokes Female-Specific Migraine Behavior. Ann Neurol *89*, 1129-1144.

Bai, L., Lehnert, B.P., Liu, J., Neubarth, N.L., Dickendesher, T.L., Nwe, P.H., Cassidy, C., Woodbury, C.J., and Ginty, D.D. (2015). Genetic Identification of an Expansive Mechanoreceptor Sensitive to Skin Stroking. Cell *163*, 1783-1795.

Belugin, S., Diogenes, A.R., Patil, M.J., Ginsburg, E., Henry, M.A., and Akopian, A.N. (2013). Mechanisms of transient signaling via short and long prolactin receptor isoforms in female and male sensory neurons. J Biol Chem *288*, 34943-34955.

Boyd, J.T., LoCoco, P.M., Furr, A.R., Bendele, M.R., Tram, M., Li, Q., Chang, F.M., Colley, M.E., Samenuk, G.M., Arris, D.A.*, et al.* (2021). Elevated dietary omega-6 polyunsaturated fatty acids induce reversible peripheral nerve dysfunction that exacerbates comorbid pain conditions. Nat Metab *3*, 762-773.

Cayrol, T., Meeus, M., Aron, V., Gatto, C., Mouraux, A., Roussel, N.A., Sallaz, L., van den Broeke, E.N., and Pitance, L. (2022). Evidence for alterations to dynamic quantitative

sensory tests in patients with chronic temporomandibular myalgia: A systematic review of observational studies with meta-analysis. J Oral Rehabil *49*, 654-670.

Chisnoiu, A.M., Picos, A.M., Popa, S., Chisnoiu, P.D., Lascu, L., Picos, A., and Chisnoiu, R. (2015). Factors involved in the etiology of temporomandibular disorders - a literature review. Clujul Med *88*, 473-478.

Davidson, J.A., Metzinger, S.E., Tufaro, A.P., and Dellon, A.L. (2003). Clinical implications of the innervation of the temporomandibular joint. J Craniofac Surg *14*, 235-239.

Day, I.N., and Thompson, R.J. (2010). UCHL1 (PGP 9.5): neuronal biomarker and ubiquitin system protein. Prog Neurobiol *90*, 327-362.

de Carvalho Santuchi, M., Dutra, M.F., Vago, J.P., Lima, K.M., Galvao, I., de Souza-Neto, F.P., Morais, E.S.M., Oliveira, A.C., de Oliveira, F.C.B., Goncalves, R.*, et al.* (2019). Angiotensin-(1-7) and Alamandine Promote Anti-inflammatory Response in Macrophages In Vitro and In Vivo. Mediators Inflamm *2019*, 2401081.

Dworkin, S.F., and Massoth, D.L. (1994). Temporomandibular disorders and chronic pain: disease or illness? J Prosthet Dent *72*, 29-38.

Ettlin, D.A., Napimoga, M.H., Meira, E.C.M., and Clemente-Napimoga, J.T. (2021). Orofacial musculoskeletal pain: An evidence-based bio-psycho-social matrix model. Neurosci Biobehav Rev *128*, 12-20.

Ferreira-Pinto, M.J., Kanodia, H., Falasconi, A., Sigrist, M., Esposito, M.S., and Arber, S. (2021). Functional diversity for body actions in the mesencephalic locomotor region. Cell *184*, 4564-4578 e4518.

Fitzcharles, M.A., Cohen, S.P., Clauw, D.J., Littlejohn, G., Usui, C., and Hauser, W. (2021). Nociplastic pain: towards an understanding of prevalent pain conditions. Lancet *397*, 2098-2110.

Furusawa, K., Yamaoka, M., Iguchi, K., and Kumai, T. (1993). Tactile-evoked response of sensory fibers in buccal and submandibular regions of the rat. Somatosens Mot Res *10*, 291-295.

He, P., Yang, X.X., He, X.Q., Chen, J., Li, F.X., Gu, X., Jiang, J.H., Liang, H.Y., Yao, G.Y., and He, J.X. (2014). CHRNA3 polymorphism modifies lung adenocarcinoma risk in the Chinese Han population. Int J Mol Sci *15*, 5446-5457.

Henry, M.A., Luo, S., and Levinson, S.R. (2012). Unmyelinated nerve fibers in the human dental pulp express markers for myelinated fibers and show sodium channel accumulations. BMC Neurosci *13*, 29.

Hockley, J.R.F., Taylor, T.S., Callejo, G., Wilbrey, A.L., Gutteridge, A., Bach, K., Winchester, W.J., Bulmer, D.C., McMurray, G., and Smith, E.S.J. (2019). Single-cell RNAseq reveals seven classes of colonic sensory neuron. Gut *68*, 633-644.

Johansson, A.S., Isberg, A., and Isacsson, G. (1990). A radiographic and histologic study of the topographic relations in the temporomandibular joint region: implications for a nerve entrapment mechanism. J Oral Maxillofac Surg *48*, 953-961; discussion 962.

Joseph, J., Qu, L., Wang, S., Kim, M., Bennett, D., Ro, J., Caterina, M.J., and Chung, M.K. (2019). Phosphorylation of TRPV1 S801 Contributes to Modality-Specific Hyperalgesia in Mice. J Neurosci *39*, 9954-9966.

Kosek, E., Cohen, M., Baron, R., Gebhart, G.F., Mico, J.A., Rice, A.S.C., Rief, W., and Sluka, A.K. (2016). Do we need a third mechanistic descriptor for chronic pain states? Pain *157*, 1382-1386.

Kristensen, K.D., Stoustrup, P., Kuseler, A., Pedersen, T.K., Twilt, M., and Herlin, T. (2016). Clinical predictors of temporomandibular joint arthritis in juvenile idiopathic arthritis: A systematic literature review. Semin Arthritis Rheum *45*, 717-732.

Kucukguven, A., Demiryurek, M.D., and Vargel, I. (2022). Temporomandibular joint innervation: Anatomical study and clinical implications. Ann Anat *240*, 151882.

Kupari, J., Usoskin, D., Parisien, M., Lou, D., Hu, Y., Fatt, M., Lonnerberg, P., Spangberg, M., Eriksson, B., Barkas, N.*, et al.* (2021). Single cell transcriptomics of primate sensory neurons identifies cell types associated with chronic pain. Nat Commun *12*, 1510.

Lawson, S.N., and Waddell, P.J. (1991). Soma neurofilament immunoreactivity is related to cell size and fibre conduction velocity in rat primary sensory neurons. J Physiol *435*, 41-63.

Lee, J.S., Zhang, Y., and Ro, J.Y. (2009). Involvement of neuronal, inducible and endothelial nitric oxide synthases in capsaicin-induced muscle hypersensitivity. Eur J Pain *13*, 924-928.

Lewis, C.M., Ni, J., Wunderle, T., Jendritza, P., Lazar, A., Diester, I., and Fries, P. (2021). Cortical gamma-band resonance preferentially transmits coherent input. Cell Rep *35*, 109083.

Li, L., Rutlin, M., Abraira, V.E., Cassidy, C., Kus, L., Gong, S., Jankowski, M.P., Luo, W., Heintz, N., Koerber, H.R.*, et al.* (2011). The functional organization of cutaneous low-threshold mechanosensory neurons. Cell *147*, 1615-1627.

Lindquist, K.A., Belugin, S., Hovhannisyan, A.H., Corey, T.M., Salmon, A., and Akopian, A.N. (2021). Identification of Trigeminal Sensory Neuronal Types Innervating Masseter Muscle. eNeuro *8*.

Manfredini, D., Guarda-Nardini, L., Winocur, E., Piccotti, F., Ahlberg, J., and Lobbezoo, F. (2011). Research diagnostic criteria for temporomandibular disorders: a systematic review of axis I epidemiologic findings. Oral Surg Oral Med Oral Pathol Oral Radiol Endod *112*, 453-462.

Marinkovic, S., Gibo, H., Todorovic, V., Antic, B., Kovacevic, D., Milisavljevic, M., and Cetkovic, M. (2009). Ultrastructure and immunohistochemistry of the trigeminal peripheral myelinated axons in patients with neuralgia. Clin Neurol Neurosurg *111*, 795-800.

Melo-Carrillo, A., Strassman, A.M., Nir, R.R., Schain, A.J., Noseda, R., Stratton, J., and Burstein, R. (2017). Fremanezumab-A Humanized Monoclonal Anti-CGRP Antibody-Inhibits Thinly Myelinated (Adelta) But Not Unmyelinated (C) Meningeal Nociceptors. J Neurosci *37*, 10587-10596.

Meloto, C.B., Slade, G.D., Lichtenwalter, R.N., Bair, E., Rathnayaka, N., Diatchenko, L., Greenspan, J.D., Maixner, W., Fillingim, R.B., and Ohrbach, R. (2019). Clinical predictors of persistent temporomandibular disorder in people with first-onset temporomandibular disorder: A prospective case-control study. J Am Dent Assoc *150*, 572-581 e510.

Mense, S. (2003). The pathogenesis of muscle pain. Curr Pain Headache Rep *7*, 419-425.

Moutafidi, A., Gatzounis, G., Zolota, V., and Assimakopoulou, M. (2021). Heat shock factor 1 in brain tumors: a link with transient receptor potential channels TRPV1 and TRPA1. J Mol Histol *52*, 1233-1244.

Navarro-Gonzalez, C., Carceller, H., Benito Vicente, M., Serra, I., Navarrete, M., Dominguez-Canterla, Y., Rodriguez-Prieto, A., Gonzalez-Manteiga, A., and Fazzari, P. (2021). Nrg1 haploinsufficiency alters inhibitory cortical circuits. Neurobiol Dis *157*, 105442.

Nguyen, M.Q., von Buchholtz, L.J., Reker, A.N., Ryba, N.J., and Davidson, S. (2021). Single-nucleus transcriptomic analysis of human dorsal root ganglion neurons. Elife *10*.

Nguyen, M.Q., Wu, Y., Bonilla, L.S., von Buchholtz, L.J., and Ryba, N.J.P. (2017). Diversity amongst trigeminal neurons revealed by high throughput single cell sequencing. PLoS One *12*, e0185543.

Nickel, J.C., Gonzalez, Y.M., Wu, Y., Liu, Y., Liu, H., and Iwasaki, L.R. (2022). Chronic Pain-Related Jaw Muscle Motor Load and Sensory Processing. J Dent Res *101*, 1165-1171.

Nonaka, N., Goto, N., Ezure, H., Ishikawa, H., and Oka, K. (2001). Unmyelinated nerve fibers of the human mandibular nerve. Okajimas Folia Anat Jpn *77*, 217-219.

Oka, K., Goto, N., Nonaka, N., Goto, J., and Tsurumi, T. (2001). Nerve fiber analysis and age-related changes of the human mandibular nerve. Okajimas Folia Anat Jpn *78*, 39-41.

Patil, M., Hovhannisyan, A.H., Wangzhou, A., Mecklenburg, J., Koek, W., Goffin, V., Grattan, D., Boehm, U., Dussor, G., Price, T.J.*, et al.* (2019). Prolactin receptor expression in mouse dorsal root ganglia neuronal subtypes is sex-dependent. J Neuroendocrinol *31*, e12759.

Patil, M.J., Hovhannisyan, A.H., and Akopian, A.N. (2018). Characteristics of sensory neuronal groups in CGRP-cre-ER reporter mice: Comparison to Nav1.8-cre, TRPV1-cre and TRPV1-GFP mouse lines. PLoS One *13*, e0198601.

Prato, V., Taberner, F.J., Hockley, J.R.F., Callejo, G., Arcourt, A., Tazir, B., Hammer, L., Schad, P., Heppenstall, P.A., Smith, E.S.*, et al.* (2017). Functional and Molecular Characterization of Mechanoinsensitive "Silent" Nociceptors. Cell Rep *21*, 3102-3115.

Ro, J.Y., and Capra, N.F. (2006). Assessing mechanical sensitivity of masseter muscle in lightly anesthetized rats: a model for craniofacial muscle hyperalgesia. Neurosci Res *56*, 119-123.

Rutlin, M., Ho, C.Y., Abraira, V.E., Cassidy, C., Bai, L., Woodbury, C.J., and Ginty, D.D. (2014). The cellular and molecular basis of direction selectivity of Adelta-LTMRs. Cell *159*, 1640-1651.

Samms, R.J., Cosgrove, R., Snider, B.M., Furber, E.C., Droz, B.A., Briere, D.A., Dunbar, J., Dogra, M., Alsina-Fernandez, J., Borner, T.*, et al.* (2022). GIPR Agonism Inhibits PYY-Induced Nausea-Like Behavior. Diabetes *71*, 1410-1423.

Seal, R.P., Wang, X., Guan, Y., Raja, S.N., Woodbury, C.J., Basbaum, A.I., and Edwards, R.H. (2009). Injury-induced mechanical hypersensitivity requires C-low threshold mechanoreceptors. Nature *462*, 651-655.

Sharma, N., Flaherty, K., Lezgiyeva, K., Wagner, D.E., Klein, A.M., and Ginty, D.D. (2020). The emergence of transcriptional identity in somatosensory neurons. Nature *577*, 392-398.

Srbely, J.Z., Dickey, J.P., Bent, L.R., Lee, D., and Lowerison, M. (2010). Capsaicin-induced central sensitization evokes segmental increases in trigger point sensitivity in humans. J Pain *11*, 636-643.

Svensson, P., and Graven-Nielsen, T. (2001). Craniofacial muscle pain: review of mechanisms and clinical manifestations. J Orofac Pain *15*, 117-145.

Tavares-Ferreira, D., Shiers, S., Ray, P.R., Wangzhou, A., Jeevakumar, V., Sankaranarayanan, I., Cervantes, A.M., Reese, J.C., Chamessian, A., Copits, B.A.*, et al.* (2022). Spatial transcriptomics of dorsal root ganglia identifies molecular signatures of human nociceptors. Sci Transl Med *14*, eabj8186.

Treede, R.D., Rief, W., Barke, A., Aziz, Q., Bennett, M.I., Benoliel, R., Cohen, M., Evers, S., Finnerup, N.B., First, M.B.*, et al.* (2015). A classification of chronic pain for ICD-11. Pain *156*, 1003-1007.

Tsuboi, Y., Honda, K., Bae, Y.C., Shinoda, M., Kondo, M., Katagiri, A., Echizenya, S., Kamakura, S., Lee, J., and Iwata, K. (2015). Morphological and functional changes in regenerated primary afferent fibres following mental and inferior alveolar nerve transection. Eur J Pain *19*, 1258-1266.

Tsuboi, Y., Takeda, M., Tanimoto, T., Ikeda, M., Matsumoto, S., Kitagawa, J., Teramoto, K., Simizu, K., Yamazaki, Y., Shima, A.*, et al.* (2004). Alteration of the second branch of the trigeminal nerve activity following inferior alveolar nerve transection in rats. Pain *111*, 323-334.

Usoskin, D., Furlan, A., Islam, S., Abdo, H., Lonnerberg, P., Lou, D., Hjerling-Leffler, J., Haeggstrom, J., Kharchenko, O., Kharchenko, P.V.*, et al.* (2015). Unbiased classification of sensory neuron types by large-scale single-cell RNA sequencing. Nat Neurosci *18*, 145-153.

Welk, E., Leah, J.D., and Zimmermann, M. (1990). Characteristics of A- and C-fibers ending in a sensory nerve neuroma in the rat. J Neurophysiol *63*, 759-766.

Wu, P., Arris, D., Grayson, M., Hung, C.N., and Ruparel, S. (2018). Characterization of sensory neuronal subtypes innervating mouse tongue. PLoS One *13*, e0207069.

Yang, L., Xu, M., Bhuiyan, S.A., Li, J., Zhao, J., Cohrs, R.J., Susterich, J.T., Signorelli, S., Green, U., Stone, J.R.*, et al.* (2022). Human and mouse trigeminal ganglia cell atlas implicates multiple cell types in migraine. Neuron *110*, 1806-1821 e1808.

Legends to Figures:

Figure 1. ***Schematic for sensory neuronal innervation of masticatory muscles***.
V1 – ophthalmic nerve; V2 – maxillary nerve; V3 – mandibular nerve; MN – masseteric nerve; ATN - auriculotemporal nerve; TN – posterior deep temporal nerve; TJM nerve – TJM branch of mandibular nerve; LPM - lateral pterygoid muscle; MM – masseter muscle; TM – temporal muscle.

Figure 2. ***Representation of pgp9.5 and NFH-positive fibers in MM, TM and LPM of adult male marmosets***.
Representative micro-photographs show relative expression of NFH (A-fibers) and pgp9.5 (all fibers) positive fibers in MM, TM, and LPM of adult male marmosets. Blue arrows indicate pgp9.5$^+$/NFH$^-$ fibers. Pictures from MM, TM and LPM, as well as antibodies used, and corresponding colors are indicated. Scales are presented in each microphotograph.

Figure 3. ***Percentages of different fiber types in MM, TM and LPM of adult male marmosets***.
(**A**) Baragraphs reflect percentages of marker-positive sensory fibers relative to NFH (A-fibers) in MM, TM, and LPM of adult male marmosets. (**B**) Baragraphs reflect percentages of GFAP$^+$ (myelinated) and TH$^+$ (sympathetic) fibers relative to NFH (A-fibers) in MM, TM, and LPM of adult male marmosets. X-axis denotes markers and tissue types (i.e. MM, TM and LPM). N=3 for MM and N=2 for TM and LPM.

Figure 4. ***Representations of myelinated fibers in MM, TM and LPM of adult male marmosets***.
Representative micro-photographs show GFAP myelinated fiber distributions relative to NFH$^+$ fibers in MM, TM, and LPM of adult male marmosets. Blue arrows indicate GFAP$^+$/NFH$^-$ fibers. Pictures from MM, TM and LPM as well as antibodies used and corresponding colors are indicated. Scales are presented in each microphotograph.

Figure 5. ***Distribution of peptidergic fibers in MM, TM and LPM of adult male marmosets***.
Representative micro-photographs show CGRP-positive peptidergic fiber distributions relative to NFH$^+$ fibers in MM, TM, and LPM of adult male marmosets. Yellow arrows indicate CGRP$^+$/NFH$^+$ fibers, cyan arrows show CGRP$^+$/NFH$^-$ fibers, and blue arrows mark CGRP$^-$/NFH$^+$ fibers. Pictures from MM, TM and LPM as well as antibodies used and corresponding colors are indicated. Scales are presented in each microphotograph.

Figure 6. ***Distribution of trpV1-, MrgprD and CHRNA3-positive fibers in MM of adult male marmosets***.
Representative micro-photographs show trpV1$^+$, mrgprD$^+$ non-peptidergic fiber, and CHRNA3$^+$, marker for "silent" nociceptors, fiber distributions relative to CGRP$^+$ and/or NFH$^+$ nerves in MM of adult male marmosets. Yellow arrows in top row panels mark CGRP$^+$/NFH$^+$/trpV1$^-$ fibers. Pictures from MM as well as antibodies used and corresponding colors are indicated. Scales are presented in each microphotograph.

Figure 7. ***Distribution of trpV1-, MrgprD and CHRNA3-positive fibers in TM and LPM of adult male marmosets***.
Representative micro-photographs show trpV1$^+$, mrgprD$^+$ and CHRNA3$^+$ fiber distributions relative to NFH$^+$ nerves in TM and LPM of adult male marmosets. Yellow arrows (panels for trpV1 and mrgprD) indicate trpV1$^+$/NFH$^+$ or mrgpr$^+$/NFH$^+$ fibers, while cyan arrows (panels for trpV1 and mrgprD) show trpV1$^-$/NFH$^+$ or mrgpr$^-$/NFH$^+$. Pictures from TM and LPM as well as antibodies used and corresponding colors are indicated. Scales are presented in each microphotograph.

Figure 8. ***Distribution of trkB, trkC and parvalbumin (PV)-positive fibers in MM of adult male marmosets***.
Representative micro-photographs show expression of markers for non-nociceptive neurons, trkB, trkC and parvalbumin (PV), in sensory fibers in MM of adult male marmosets. NFH was used to outline all A-fibers in the tissues. Yellow arrows in the top row panels indicate $trkB^+/NFH^+$ fibers, while cyan arrows show $trkB^-/NFH^+$ fibers. Yellow arrows in the middle row panels indicate $trkC^+/NFH^+$ fibers, . Yellow arrows in the bottom row panels indicate PV^+/NFH^+ fibers, while cyan arrows show PV^-/NFH^+ fibers. Pictures from MM as well as antibodies used and corresponding colors are indicated. Scales are presented in each microphotograph.

Figure 9. ***Distribution of trkB, trkC and parvalbumin (PV)-positive fibers in TM and LPM of adult male marmosets***.
Representative micro-photographs show expression of trkB, trkC and PV sensory fibers in TM and LPM of adult male marmosets. NFH was used to outline all A-fibers in the tissues. Yellow arrows show and $trkC^{+/}NFH^+$ (middle panels) and PV^+/NFH^+ (bottom panels) sensory fibers, while cyan arrows mark $trkB^-/NFH^+$ (top panels), $trkC^{-/}NFH^+$ (middle panels) and PV^-/NFH^+ (bottom panels) sensory fibers. Pictures from TM and LPM as well as antibodies used and corresponding colors are indicated. Scales are presented in each microphotograph.

Figure 10. ***Location of sympathetic fibers in MM, TM and LPM of adult male marmosets***.
Representative micro-photographs show the location of tyrosine hydroxylase (TH)-positive sympathetic fibers relative to blood vessels outlined with smooth muscle marker alpha-smooth muscle actin (α-SMA) and sensory A-fibers labeled with NFH in MM, TM, and LPM of adult male marmosets. Pictures from MM, TM and LPM as well as antibodies used and corresponding colors are indicated. Scales are presented in each microphotograph.

Figure 11. ***Schematic for sensory neuron subtypes and marker expression in masticatory muscles***.
Masticatory muscles type (i.e. MM, TM and LPM) are indicated from left. Sensory nerve groups innervating MM, TM or LPM are marked by lines and corresponding marker. *?* indicates unclear presence of mrgprD and trpV1 markers.

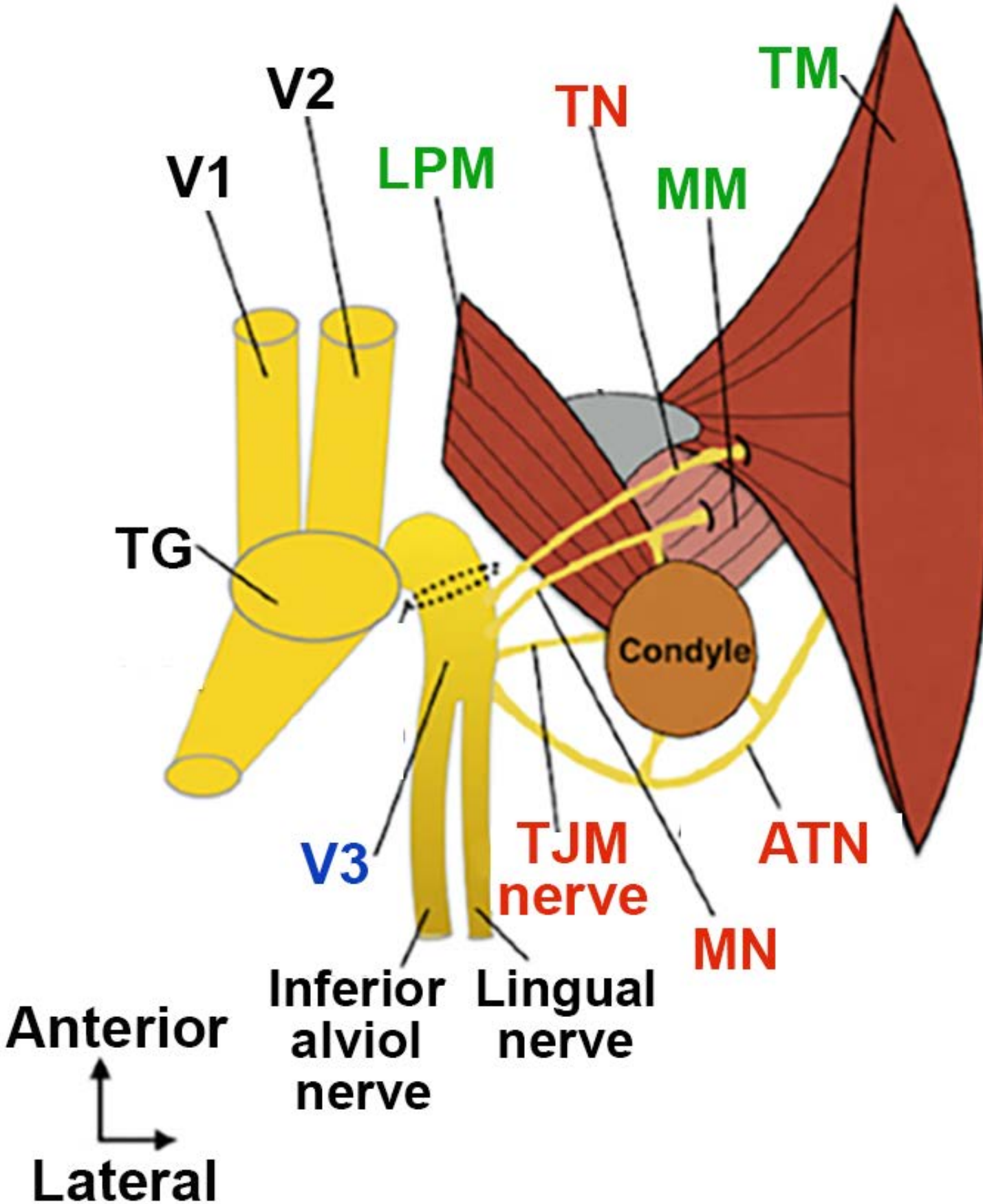
V2
V1
LPM
TN
TM
MM
TG
Condyle
V3
TJM
nerve
ATN
MN
Inferior
alviol
nerve
Lingual
nerve
Anterior
Lateral

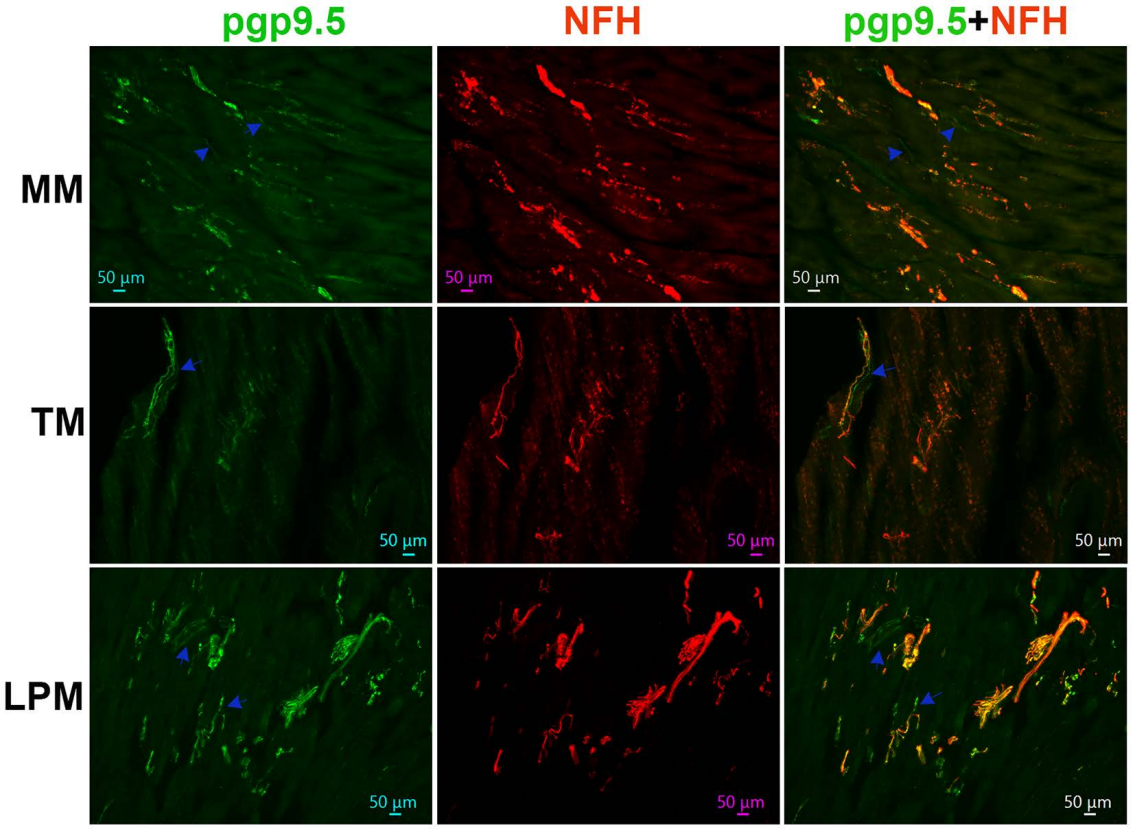
pgp9.5
NFH
pgp9.5+NFH
MM
TM
LPM
50 µm

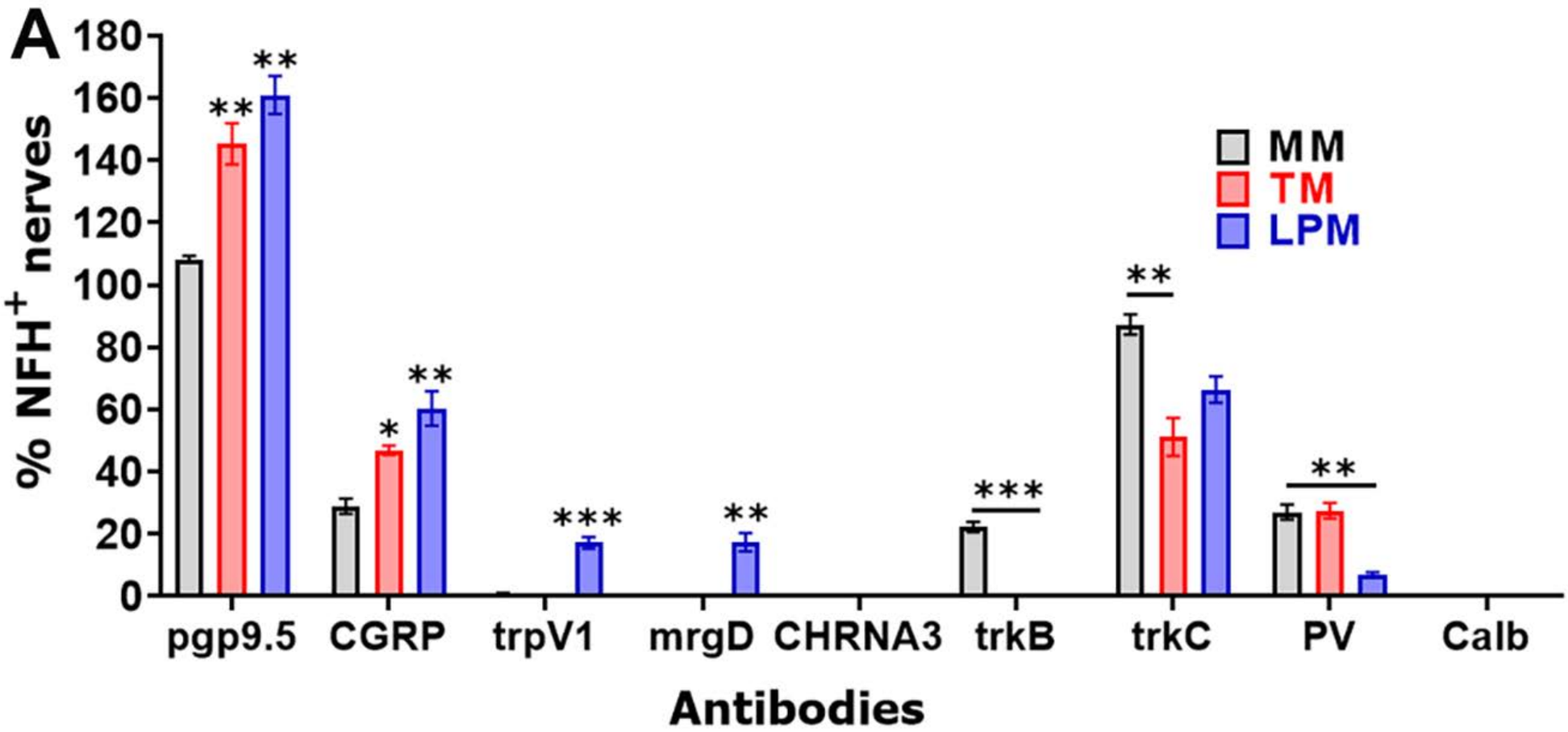
A
% NFH+ nerves
180
160
140
120
100
80
60
40
20
0
MM
TM
LPM
**
**
*
**
***
**
***
**
**
pgp9.5
CGRP
trpV1
mrgD
CHRNA3
trkB
trkC
PV
Calb
Antibodies

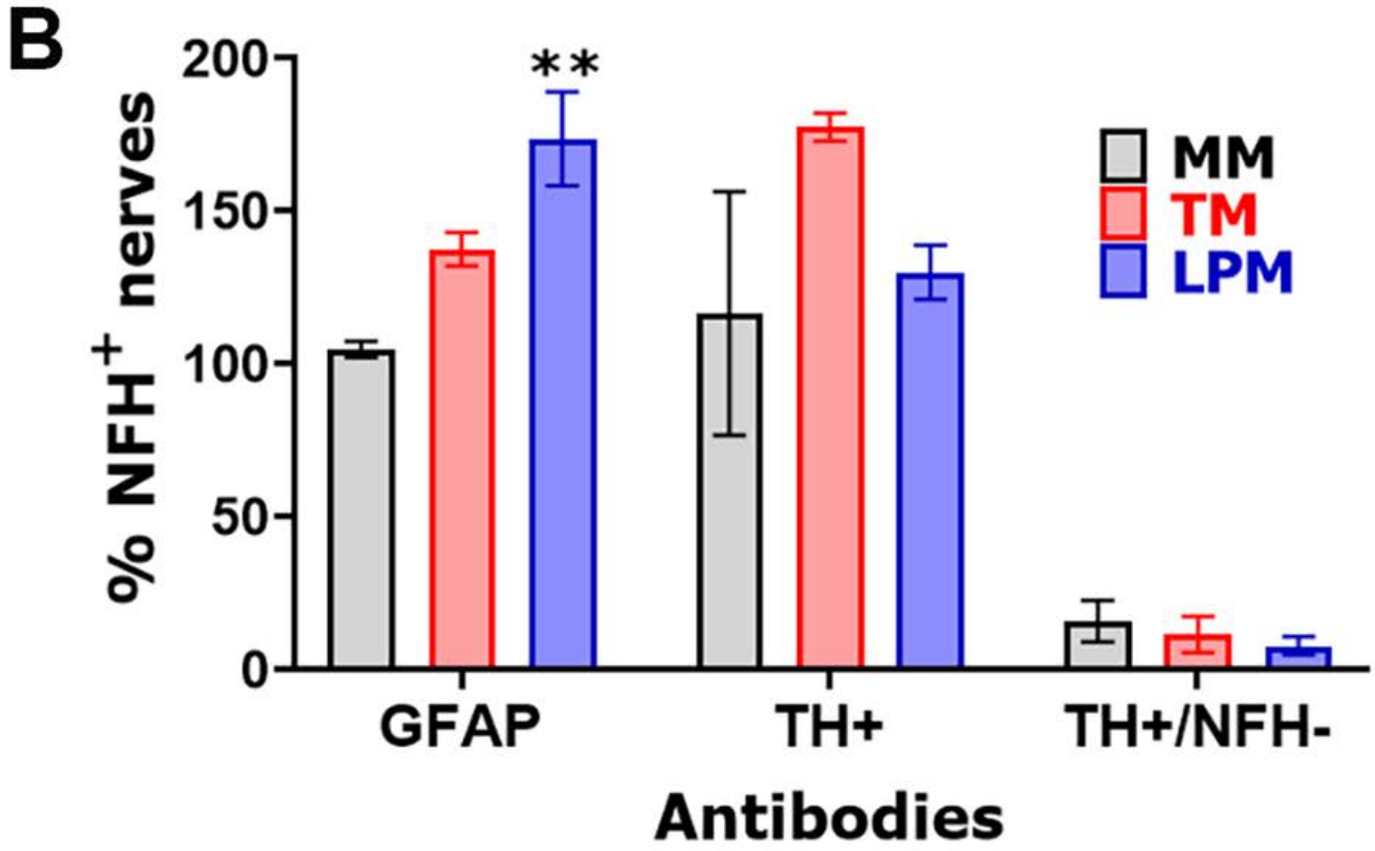
B
% NFH+ nerves
200
150
100
50
0
**
MM
TM
LPM
GFAP
TH+
TH+/NFH-
Antibodies

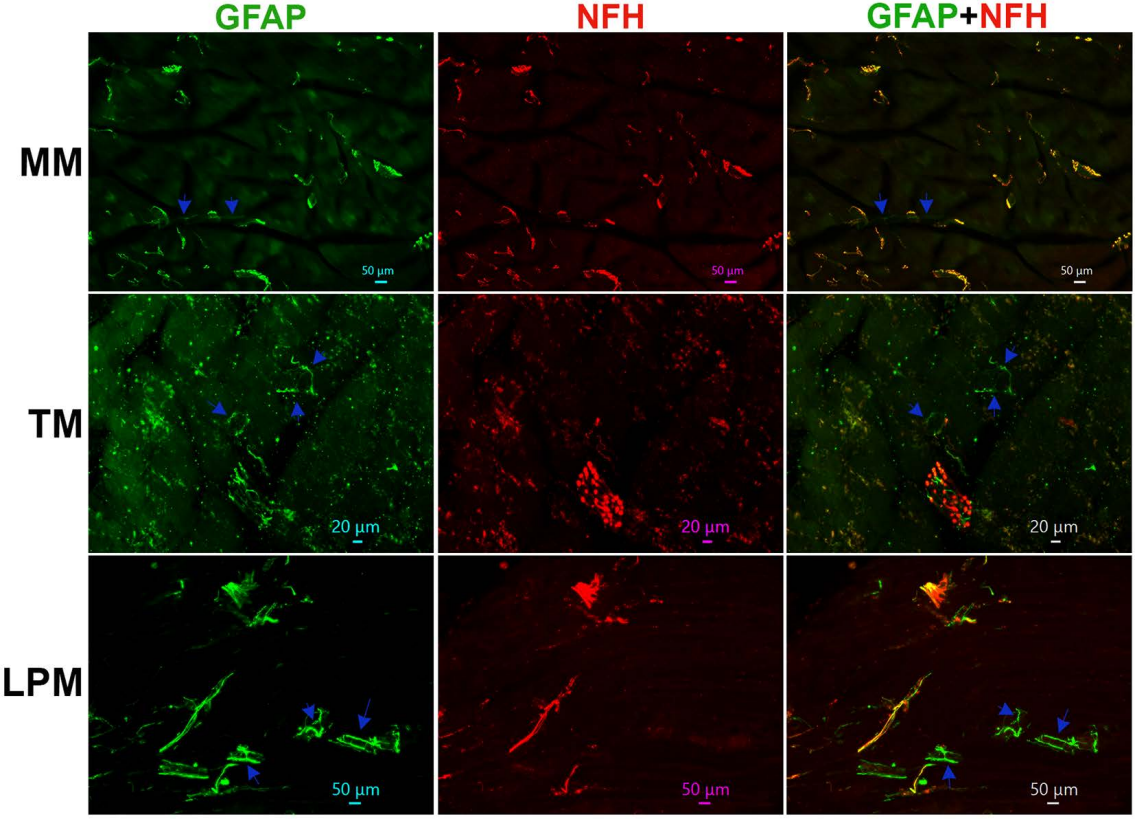
GFAP
NFH
GFAP+NFH
MM
TM
LPM
50 µm
50 µm
50 µm
20 µm
20 µm
20 µm
50 µm
50 µm
50 µm

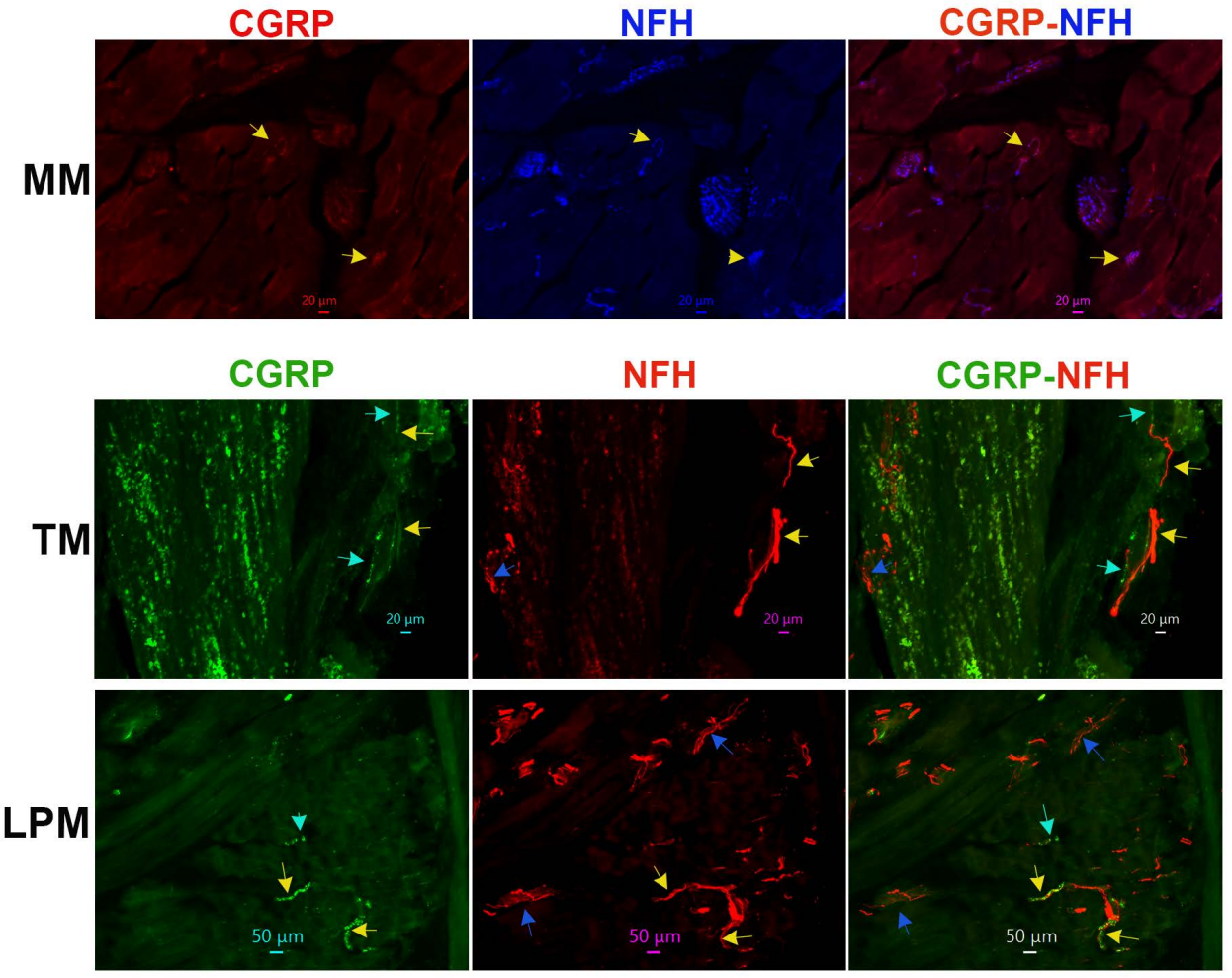
CGRP
NFH
CGRP-NFH
MM
20 µm
20 µm
20 µm
CGRP
NFH
CGRP-NFH
TM
20 µm
20 µm
20 µm
LPM
50 µm
50 µm
50 µm

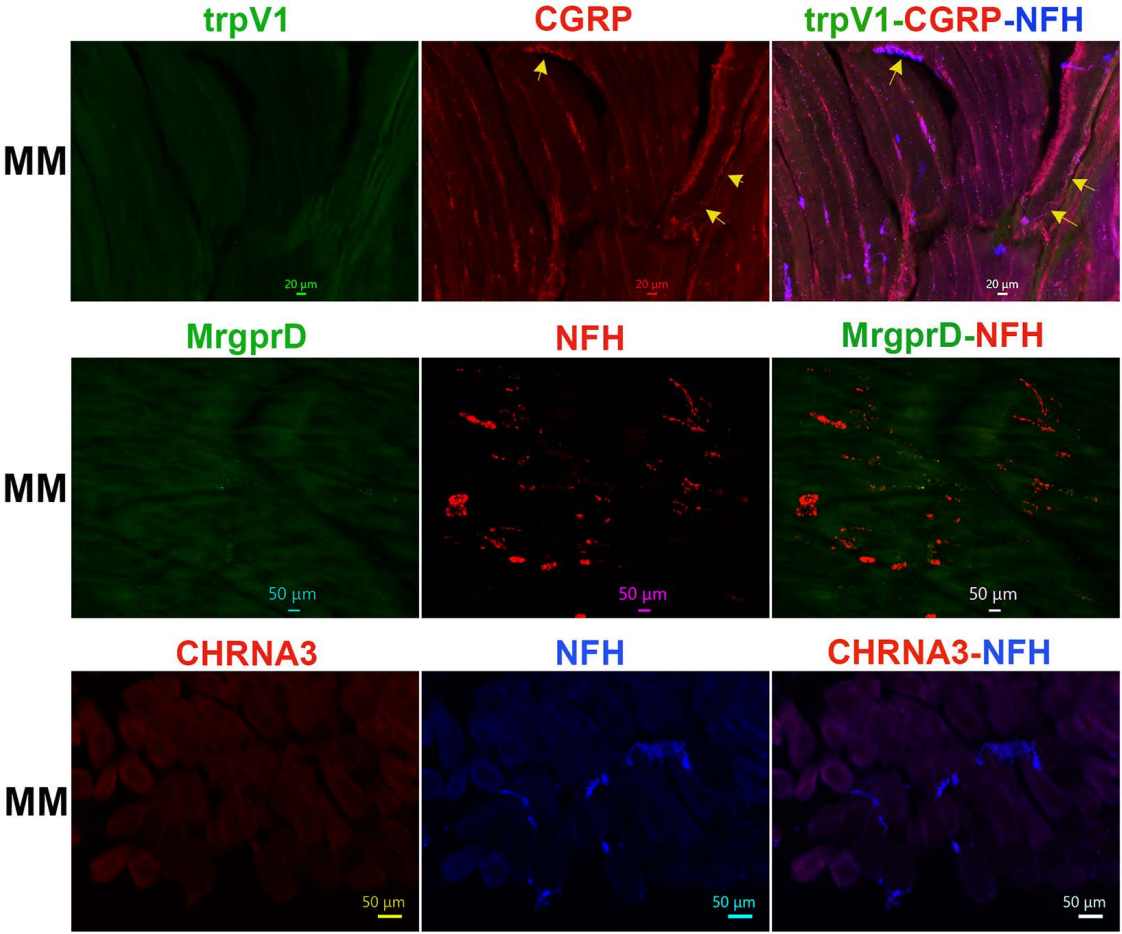
trpV1
CGRP
trpV1-CGRP-NFH
MM
20 µm
20 µm
20 µm
MrgprD
NFH
MrgprD-NFH
MM
50 µm
50 µm
50 µm
CHRNA3
NFH
CHRNA3-NFH
MM
50 µm
50 µm
50 µm

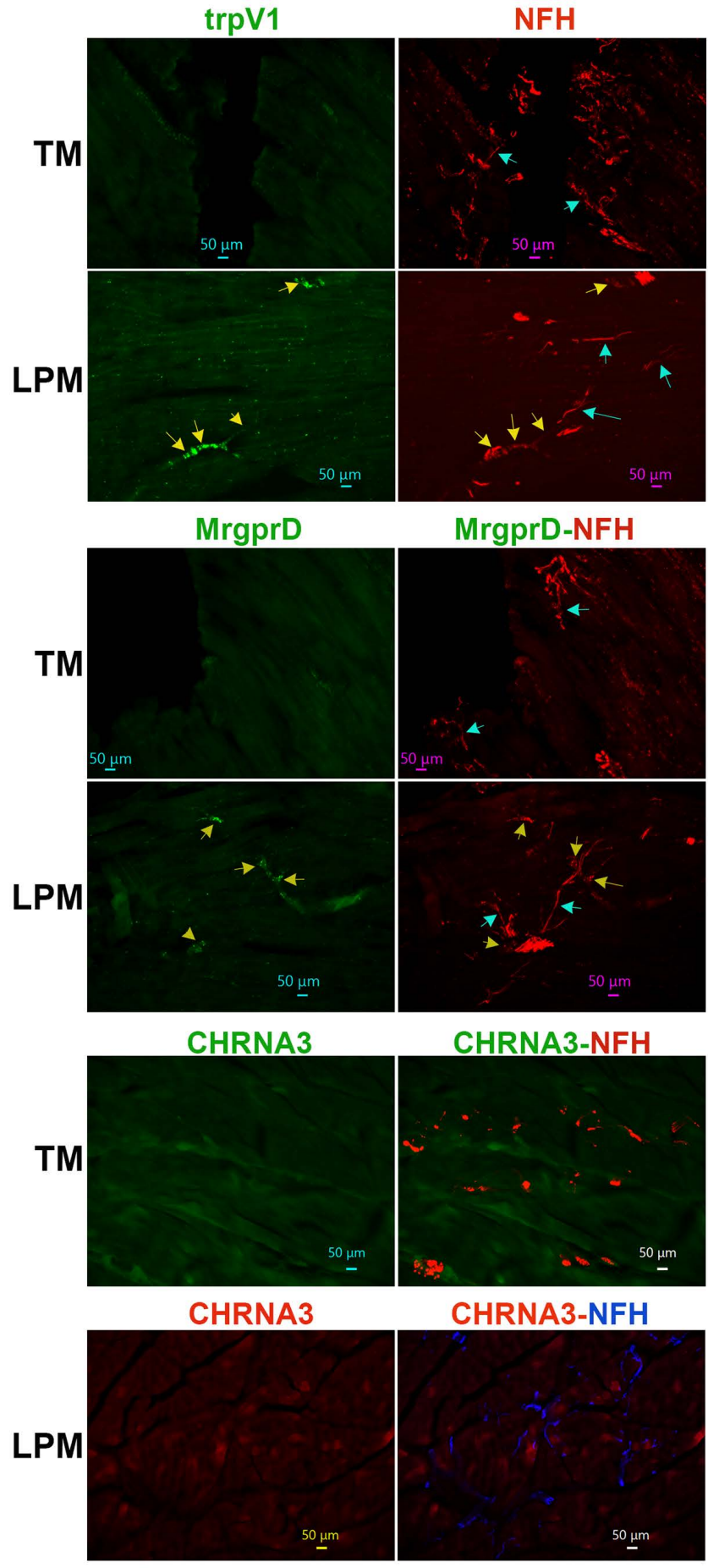
trpV1
NFH
TM
LPM
50 µm
MrgprD
MrgprD-NFH
CHRNA3
CHRNA3-NFH
CHRNA3-NFH

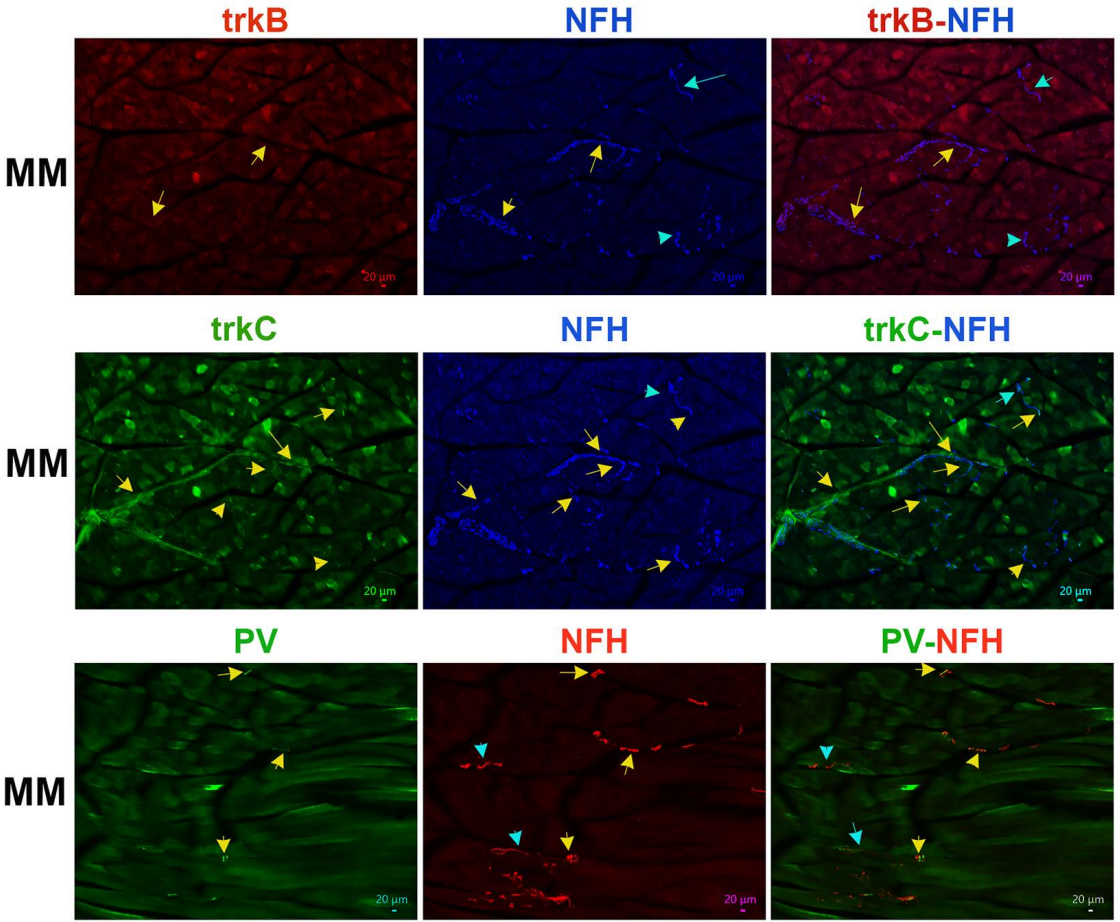
trkB
NFH
trkB-NFH
MM
20 µm
trkC
NFH
trkC-NFH
MM
20 µm
PV
NFH
PV-NFH
MM
20 µm

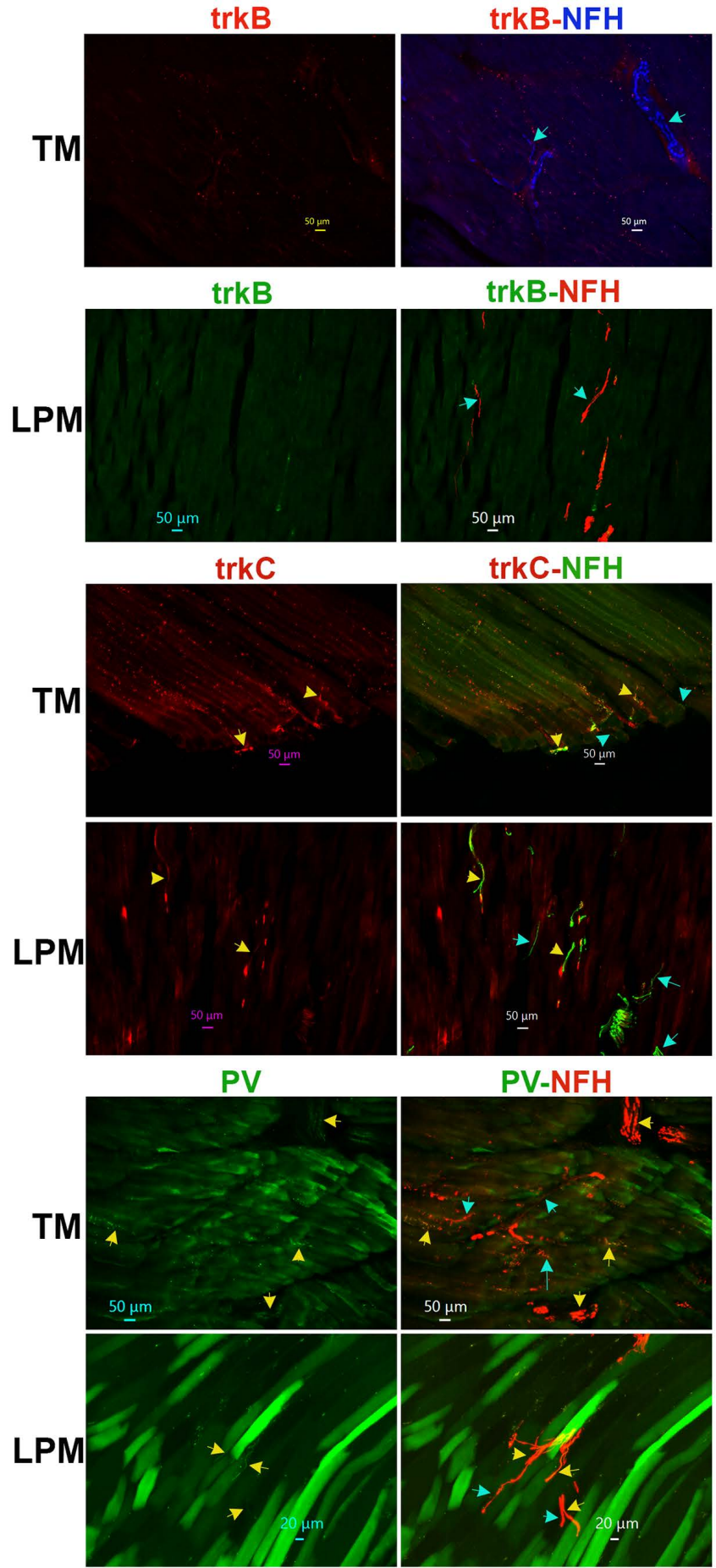
trkB
trkB-NFH
TM
50 µm
50 µm
trkB
trkB-NFH
LPM
50 µm
50 µm
trkC
trkC-NFH
TM
50 µm
50 µm
LPM
50 µm
50 µm
PV
PV-NFH
TM
50 µm
50 µm
LPM
20 µm
20 µm

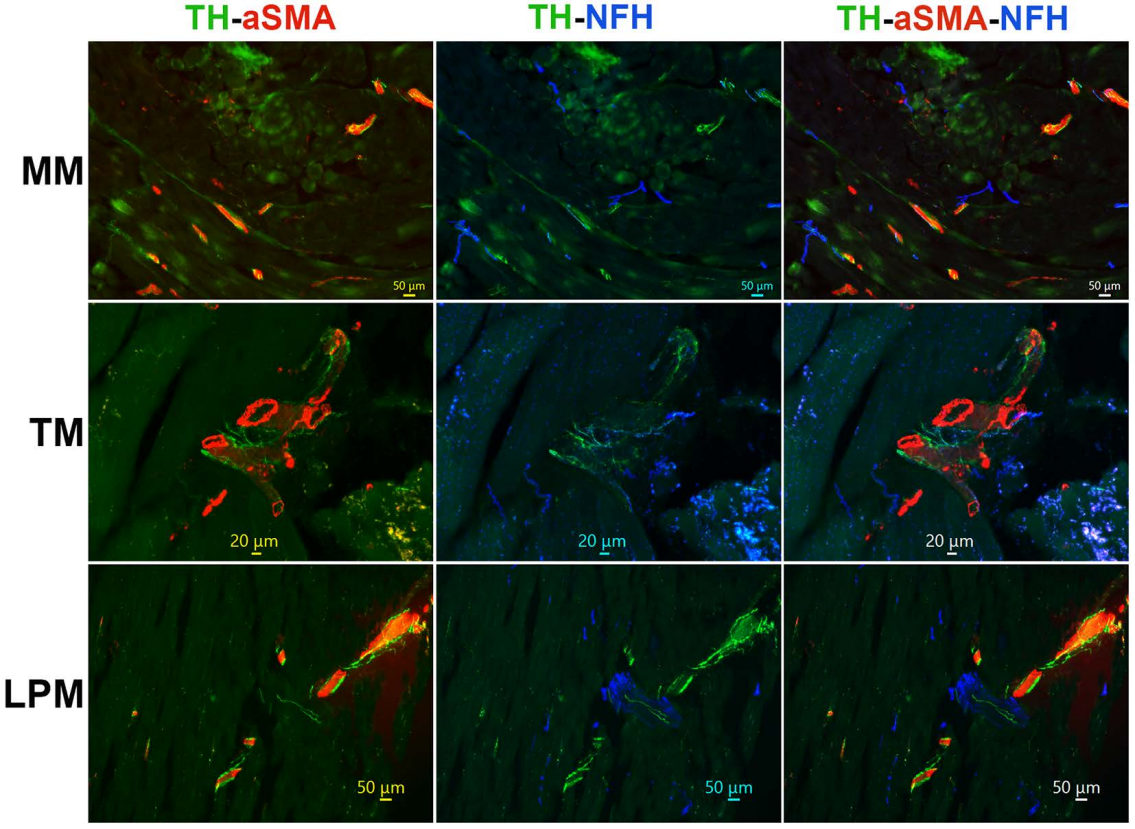
TH-aSMA
TH-NFH
TH-aSMA-NFH
MM
TM
LPM
50 µm
20 µm

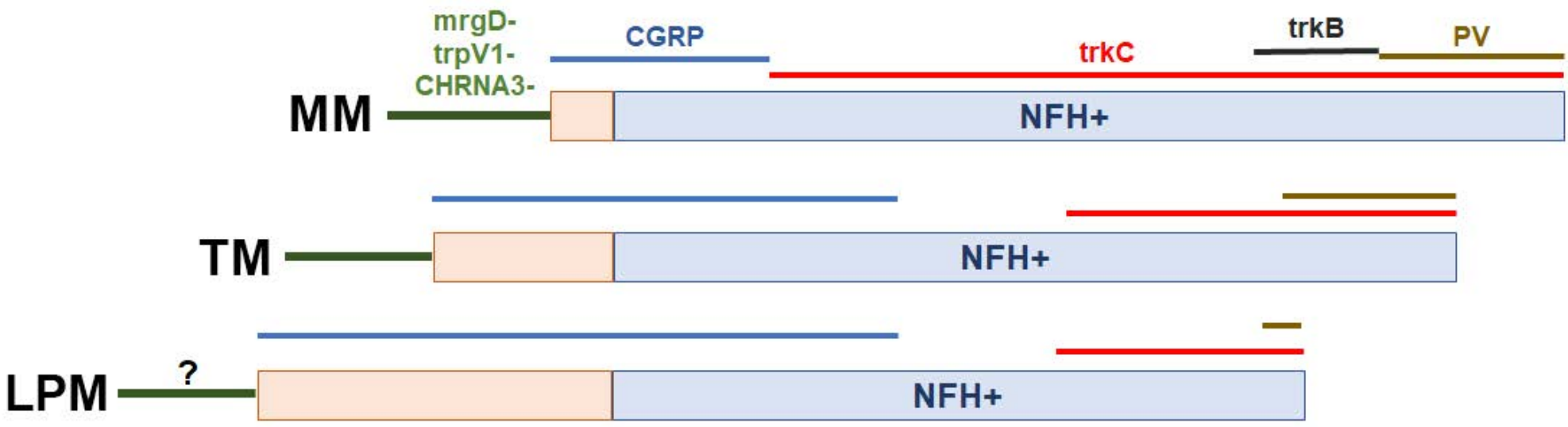
mrgD-
trpV1-
CHRNA3-
CGRP
trkC
trkB
PV
MM
NFH+
TM
NFH+
LPM
?
NFH+

Legends to Supplementary Figures:

Supplementary Figure 1. ***Positive control experiments with antibodies for nociceptors, "small" sensory neurons, and glia***.

Top-row panels show expression of CGRP (peptidergic neurons) and trpV1 in TG of adult male marmoset. *Middle row panels* show expression of GFAP (pan glial marker), mrgprD (a marker for non-peptidergic neurons) and tyrosine hydroxylase (TH; a marker for C-fiber low threshold mechanoreceptor (C-LTMR)) in in TG of adult male marmoset. *Bottom row panel* exhibits location of CHRNA3 (a marker of "silent" nociceptors in DRG) in tongue of adult male marmosets. Yellow arrows mark CHRNA3$^+$ fibers in a marmoset tongue section labeled with CHRNA3 and NFH. Antibodies used and corresponding colors are indicated. Scales are presented in microphotographs from top two rows.

Supplementary Figure 2. ***Positive control experiments with antibodies for "large, non-nociceptive neurons.***

Top-row panels show expression of trkB (a marker for Aδ-LTMR in DRG) relative to CGRP$^+$ neurons in marmoset TG, and Calbindin-1 (Calb; a marker for subset of Aβ-LTMR in DRG) in marmoset TG. *Bottom-row panels* present expressions of trkC (a marker for Aβ-LTMR in DRG) in marmoset TG, and parvalbumin (PV; a marker for a subset of Aβ-LTMR in DRG) relative to CGRP$^+$ neurons in marmoset TG. Antibodies used and corresponding colors are indicated. Scales are presented in microphotographs for trkC and Calb.

Supplementary Figure 3. ***TrkC fiber expression in TM.***

This is an example of trkC$^+$/NFH$^+$ (cyan arrows) and trkC$^-$/NFH$^+$ (yellow arrows) sensory fiber expression in TM muscle and tendon tissues. Antibodies used and corresponding colors are indicated. Scales are presented in microphotographs.

Top-row panels show expressions of trkB (a marker for Aδ-LTMR in DRG) relatively to $CGRP^+$ neurons in marmoset TG, and Calbindin-1 (Calb; a marker for subset of Aβ-LTMR in DRG) in marmoset TG.

CGRP

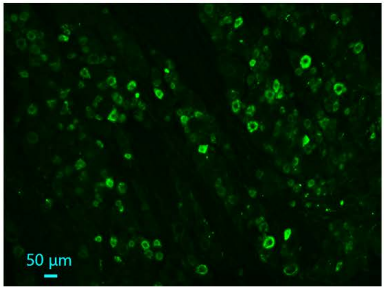

trpV1

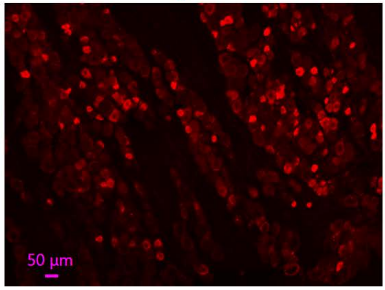

CGRP-trpV1

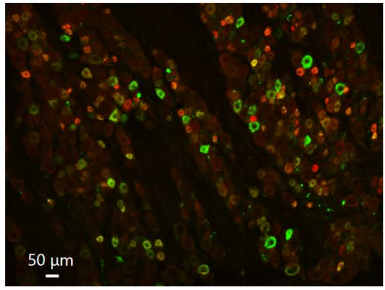

GFAP

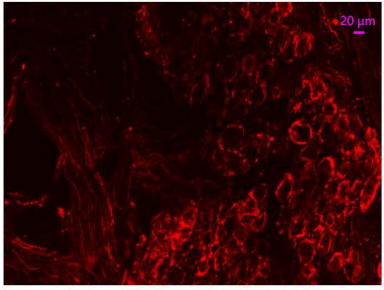

MrgprD

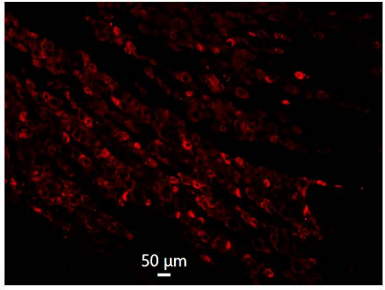

TH

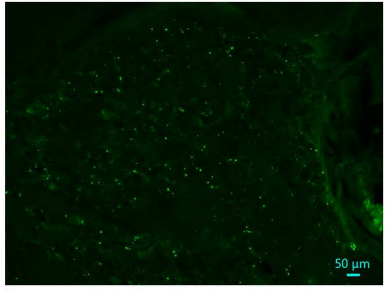

CHRNA3-NFH

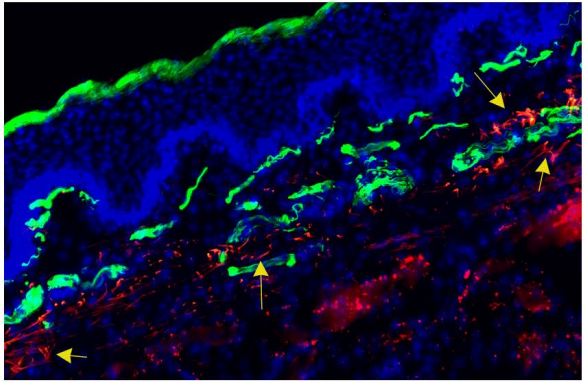

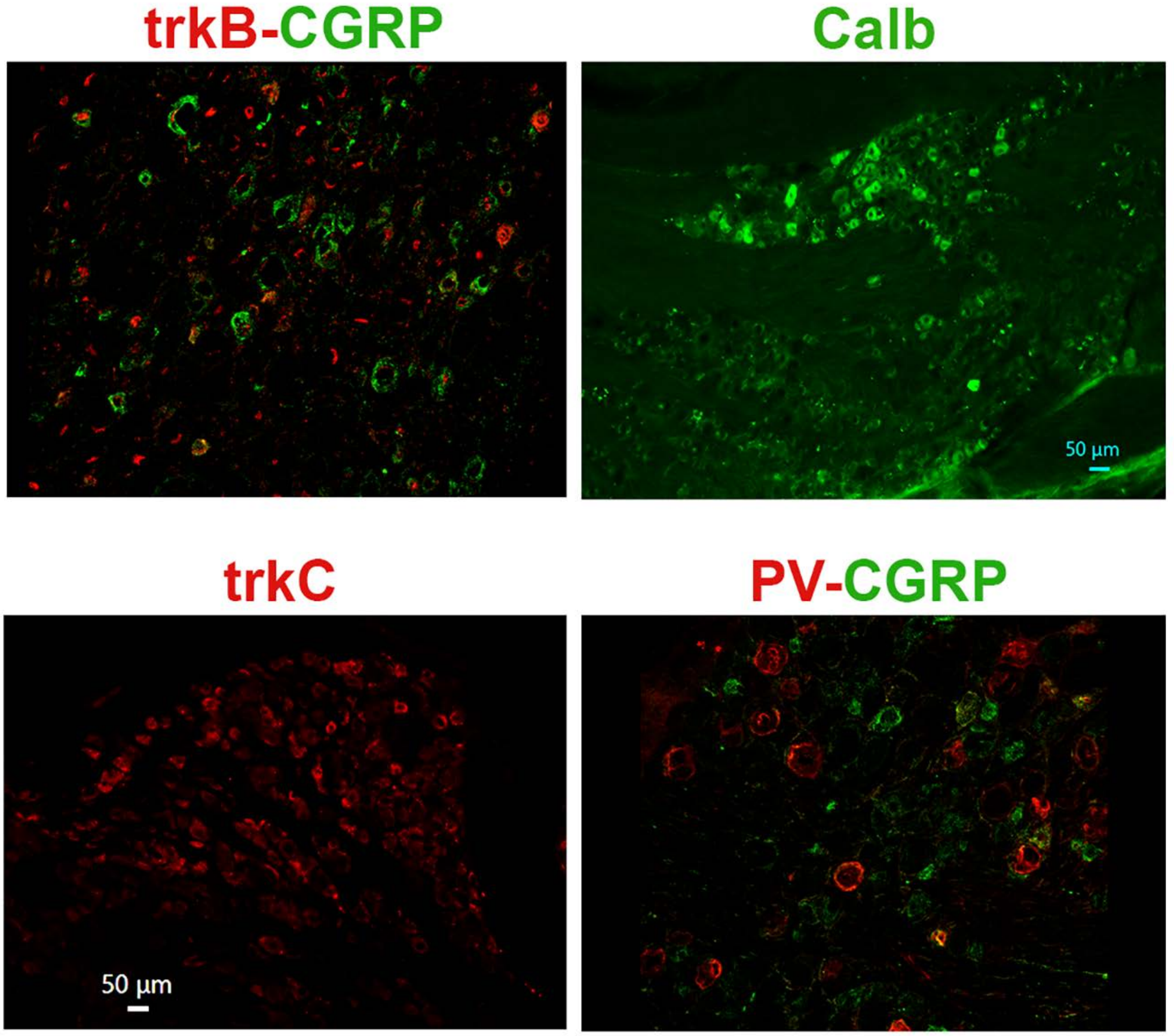
trkB-CGRP
Calb
50 µm
trkC
50 µm
PV-CGRP

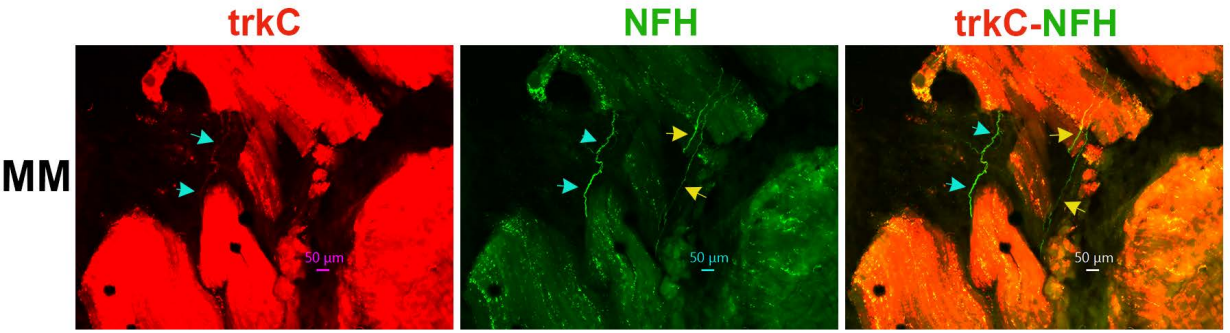
trkC
NFH
trkC-NFH
MM
50 µm
50 µm
50 µm